FOXM1 is a molecular determinant of the mitogenic and invasive phenotype of anaplastic thyroid carcinoma

Roberto Bellelli[1,2], **Maria Domenica Castellone**[1,2], **Ginesa Garcia-Rostan**[3], **Clara Ugolini**[4], **Carmelo Nucera**[5], **Peter M Sadow**[6], **Tito Claudio Nappi**[1,2], **Paolo Salerno**[1,2], **Maria Carmela Cantisani**[1,2], **Fulvio Basolo**[4], **Tomas Alvarez Gago**[3], **Giuliana Salvatore**[7], and **Massimo Santoro**[1,2]

[1]Dipartimento di Biologia e Patologia Cellulare e Molecolare, 'L. Califano', Universita' Federico II, Napoli, Italy

[2]Istituto di Endocrinologia ed Oncologia Sperimentale 'G. Salvatore', C.N.R., Napoli, Italy

[3]Institute of Biology and Molecular Genetics, Spanish Research Council, Valladolid University, Valladolid, Spain

[4]Department of Surgery, University of Pisa, Pisa, Italy

[5]Human Thyroid Cancers Preclinical and Translational Research Program, Division of Cancer Biology and Angiogenesis, Harvard Medical School, Center for Vascular Biology Research, Beth Israel Deaconess Medical Center, Boston, Massachusetts, USA

[6]Department of Pathology, Harvard Medical School, Massachusetts General Hospital, Boston, Massachusetts, USA

[7]Dipartimento di Studi delle Istituzioni e dei Sistemi Territoriali, Università Parthenope, Napoli, Italy

Abstract

Anaplastic thyroid carcinoma (ATC) is a very aggressive thyroid cancer. forkhead box protein M1 (FOXM1) is a member of the forkhead box family of transcription factors involved in control of cell proliferation, chromosomal stability, angiogenesis, and invasion. Here, we show that FOXM1 is significantly increased in ATCs compared with normal thyroid, well-differentiated thyroid carcinomas (papillary and/or follicular), and poorly differentiated thyroid carcinomas (P=0.000002). Upregulation of FOXM1 levels in ATC cells was mechanistically linked to loss-of-function of p53 and to the hyperactivation of the phosphatidylinositol-3-kinase/AKT/FOXO3a pathway. Knockdown of FOXM1 by RNA interference inhibited cell proliferation by arresting cells in G2/M and reduced cell invasion and motility. This phenotype was associated with decreased expression of FOXM1 target genes, like cyclin B1 (*CCNB1*), polo-like kinase 1 (*PLK1*), Aurora B (*AURKB*), S-phase kinase-associated protein 2 (*SKP2*), and plasminogen activator, urokinase: uPA (*PLAU*). Pharmacological inhibition of FOXM1 in an orthotopic mouse model of ATC reduced tumor burden and metastasization. All together, these findings suggest that FOXM1 represents an important player in thyroid cancer progression to the anaplastic phenotype and a potential therapeutic target for this fatal cancer.

Introduction

Anaplastic thyroid carcinoma (ATC) is a rare tumor that accounts for 2–5% of all thyroid cancers. ATC ranks among the most lethal solid malignancies with a mean survival rate of 4–12 months after diagnosis. ATC usually presents between the 6th and the 7th decade of life as a rapidly enlarging neck mass that extends locally and disseminates to regional nodes and distant sites. Multimodal therapy, including surgery, chemotherapy, and radiotherapy, has only limited benefits in the locoregional control of the disease (Kondo *et al.* 2006, Smallridge *et al.* 2009).

ATCs share genetic alterations with well-differentiated thyroid carcinoma (WDTC; papillary thyroid carcinoma (PTC) or follicular thyroid carcinoma (FTC)) and poorly differentiated thyroid carcinoma (PDC), namely point mutations in *RAS* and *BRAF* (Garcia-Rostan *et al.* 2003, Nikiforova *et al.* 2003). Activation of the phosphatidylinositol-3-kinase (PI3K) pathway, with point mutation or gene amplification of *PIK3CA* or *AKT* and loss of *PTEN*, is more frequently found in ATCs than in WDTCs (Gimm *et al.* 2000,Frisk *et al.* 2002, Garcia-Rostan *et al.* 2005, Wu *et al.* 2005, Santarpia *et al.* 2008, Ricarte-Filho *et al.* 2009, Saji & Ringel 2010). Accordingly, intercross of transgenic mice expressing oncogenic *Ras* with *Pten null* mice gave rise to highly aggressive ATCs (Miller *et al.* 2009). Moreover, while WDTCs are rarely associated with *Tp53* mutation, ATCs feature *Tp53* mutations (67–88%) or dysfunction (Kondo *et al.* 2006, Smallridge *et al.* 2009, Nikiforov & Nikiforova 2011).

At a variance from WDTC, ATC has a high proliferation rate and marked aneuploidy (Wreesmann *et al.* 2002). Recently, we identified a gene expression signature associated with this ATC phenotype (Salvatore *et al.* 2007). This signature included upregulation of forkhead box protein M1 (FOXM1).

FOXM1 is a member of the forkhead box family of transcription factors (Korver *et al.* 1997). It promotes cell cycle progression by affecting both the G1/S and the G2/M transitions, and it is an important regulator of chromosomal stability (Laoukili *et al.* 2005). Accordingly, FOXM1 regulates the expression of a large number of G2/M-specific genes, such as cyclin B1 (*CCNB1*), polo-like kinase 1 (*PLK1*), never in mitosis gene-related kinase 2 (*NEK2*), and centromere protein F (*CENPF*). Interestingly, most of these genes were part of the ATC signature (Salvatore *et al.* 2007) and one of them, *PLK1*, was shown to be a promising therapeutic target for ATC (Nappi *et al.* 2009). FOXM1 deletion is associated with mitotic spindle defects and cell death through mitotic catastrophe (Wonsey & Follettie 2005). Compounds, like the antibiotic thiostrepton, targeting FOXM1 induce apoptosis in cancer cell lines, suggesting that FOXM1 may represent a potential therapeutic cancer target (Bhat *et al.* 2009, Hegde *et al.* 2011). FOXM1 has also been shown to regulate the transcription of genes involved in angiogenesis and invasion, thus acting as a master regulator of metastasization (Raychaudhuri & Park 2011). Accordingly, FOXM1 downregulation reduced invasion and migration of pancreatic and breast cancer-derived cell lines (Wang *et al.* 2007, Ahmad *et al.* 2010). FOXM1 overexpression has been observed in several human cancers, including glioblastoma (Liu *et al.* 2006), basal cell (Teh *et al.* 2002), hepatocellular (Kalinichenko *et al.* 2004), breast (Wonsey & Follettie 2005), prostate (Kalin *et al.* 2006), and gastric (Li *et al.* 2009) carcinomas, being frequently associated with high proliferative rates, invasive phenotype, and dismal prognosis.

Recently, Ahmed *et al.* (2012) reported that FOXM1 was upregulated in a fraction (28.4%) of PTCs. Moreover, chemical or genetic FOXM1 block reduced PTC cell invasiveness, survival, and metalloproteinase (MMP2 and MMP9) expression levels.

Here, we show that FOXM1 is strongly upregulated in ATCs. We also show that *FOXM1* expression in ATC cells is sustained by the PI3K/AKT as well as by the loss-of-function of the p53 pathway. *FOXM1* knockdown reduced proliferation, survival, and invasion of ATC cells. Finally, pharmacological inhibition of FOXM1 reduced tumor burden and metastasization in an orthotopic mouse model of ATC. These results suggest that ATC cells are addicted to FOXM1 and that FOXM1 targeting may represent a strategy for the treatment of ATCs.

Materials and methods

Tissue samples and immunohistochemistry

Formalin-fixed paraffin-embedded ATC, PDC, and normal thyroid tissue samples (132 cases and 552 tissue cores) for immunohistochemical analysis were retrieved from the files of the Pathology Departments of Hospital Central de Asturias (Oviedo University, Asturias, Spain) and Hospital Clinico Universitario Santiago Compostela (Santiago de Compostela University, Galicia, Spain). An additional group of WDTC (36 PTCs and ten FTCs) tissue samples were retrieved from the files of the Department of Surgery, University of Pisa (Italy). Processing of samples and patient information proceeded in agreement with review board approved protocols. Case selection was based on the histological findings and availability of adequate material for RNA extraction. All histological diagnoses were reviewed by two blinded pathologists (G Garcia-Rostan and C Ugolini) according to the latest recommendations about diagnostic features of PTC, FTC, PDC, and ATC (Hedinger *et al.* 1989, Volante *et al.* 2007, Garcia-Rostan & Sobrinho-Simoes 2011). Twenty-seven percent of the PDCs (21/78) analyzed disclosed intratumoral progression, with concurrent WDTC areas (PTC or FTC in 19 or two samples respectively). Twenty-four percent (24.4%) of the ATCs (10/41) featured concurrent PDC (four cases), PTC (three cases), FTC (one case), or PDC and PTC (two cases) areas. Whenever observed, such areas with different degree of differentiation and/or aggressiveness within the same case were individually analyzed. Formalin-fixed and paraffin-embedded 3–5 µm-thick tissue microarray (TMA) sections were deparaffinized, placed in a solution of absolute methanol and 0.3% hydrogen peroxide for 30 min, and treated with blocking serum for 20 min. The slides were incubated with rabbit polyclonal anti-FOXM1 antibody (dilution 1:200; H-300, Santa Cruz Biotechnology, Santa Cruz, CA, USA) and processed according to standard procedures. Negative controls by omitting the primary antibody were included. To improve the representativity of the expression analysis, two to six core biopsies of 1 mm in diameter, from different regions of the same specimen or different blocks of the same tumor, were included in the TMAs. Cases were scored as positive when unequivocal brown staining was observed in the nuclei of tumor cells. Immunoreactivity was expressed as the average percentage of positively stained target cells (—: no staining, <5% positive cells; +: low/ weak, 5– 25% positive cells; ++: medium/moderate, >25–<50% positive cells; +++: high/ strong, 50 positive cells). Score values were independently assigned by two blinded investigators (G Garcia-Rostan and C Ugolini) and a consensus was reached on all scores used for computation.

RNA extraction and RT-PCR

Snap-frozen thyroid tumors and normal thyroid (from patients who underwent neck dissection for other diseases) tissue samples (61 cases) for RNA extraction and RT-PCR were retrieved from the files of the Department of Surgery, University of Pisa (Italy). RNA was isolated using' the RNeasy Kit (Qiagen). The quality of the RNAs was verified by the 2100 Bioanalyzer (Agilent Technologies, Waldbronn, Germany); only samples with RNA integrity number value >7 were used for further analysis. RNA (1 µg) from each sample was reverse transcribed with the QuantiTect Reverse Transcription (Qiagen). PCR reactions were

done in triplicate and fold changes were calculated with the formula:
$2^{-(\text{sample 1 } \Delta Ct - \text{sample 2 } \Delta Ct)}$, where ΔCt is the difference between the amplification
fluorescent threshold of the mRNA of interest and the mRNA of RNA polymerase 2 used as
an internal reference. Primers and PCR conditions are listed in Supplementary Materials and
Methods, see section on supplementary data given at the end of this article.

Cell cultures

Normal thyroid P5 cells were provided by F Curcio (Università di Udine, Udine, Italy) in
2003. All the other cell lines are derived from primary ATCs. 8505C and CAL62 cells were
purchased from Deutsche Sammlung von Mikroorganismen und Zellkulturen (DSMZ)
GmbH, Braunschweig, Germany) in 2006. HTH74 cells were obtained from N E Heldin
(University Hospital, Uppsala, Sweden) in 2005. OCUT-2, TTA1, and ACT1 cells were
provided by N Onoda (Osaka University of Medicine, Osaka, Japan) in 2005. All the cells
were DNA profiled by short tandem repeat analysis and shown to be unique and identical to
those reported in Schweppe *et al.* (2008). P5 were grown as described previously (Curcio *et
al.* 1994). The thyroid cancer cell lines were grown in DMEM (Invitrogen) containing 10%
fetal bovine serum. LY294002 was from Calbiochem (Merck Chemicals Ltd.) and used at
10 μM final concentration. PD98059 was from Cell Signaling (Beverly, MA, USA) and
used at 50 μM final concentration. Thiostrepton was from Sigma–Aldrich.

Protein studies

Protein extraction and immunoblotting was carried out according to standard procedures.
Anti-FOXM1 antibody (H-300) was from Santa Cruz Biotechnology; anti-cleaved (Asp[175])
caspase-3 was from Cell Signaling; anti-poly(ADP-ribose) polymerase (anti-PARP)
monoclonal antibody, which detects full-length PARP and the large fragment (89 kDa)
produced by caspase cleavage, was from BD Biosciences (San Jose, CA, USA); monoclonal
anti-α-tubulin was from Sigma–Aldrich. Secondary anti-mouse and anti-rabbit antibodies
coupled to HRP were from Santa Cruz Biotechnology.

Plasmids

The HA-FOXM1b plasmid was purchased from Origene Technologies (Rockville, MD,
USA); HA-FOXM1c was a kind gift of Dr K M Yao (University of Hong Kong). Expression
vectors for wild-type p53, p53-R248G, p21(CIP1/WAF1) (*CDKN1A*), E2F1 (1–374), E2F4,
wild-type AKT, AKT-K179M, and FOXO3a were used.

RNA interference

FOXM1 siRNA smart pool was purchased from Dharmacon (Lafayette, CO, USA). The
siCONTROL non-targeting pool (#D-001206-13-05) was used as a negative control. Cells
were transfected with 100 nM siRNA using Dharmafect 3 siRNA reagent following
manufacturer's instructions.

Invasion assay

In vitro invasiveness through Matrigel was assayed using transwell cell culture chambers.
Briefly, 8505C and HTH74 confluent cell monolayers were harvested with trypsin/EDTA
and centrifuged at 800 g for 10 min. The cell suspension (1×10^5 cells/well) was added to the
upper chamber of transwells on prehydrated polycarbonate membrane filter of 8 μm pore
size (Costar, Cambridge, MA, USA) coated with 35 μg Matrigel (BD Biosciences). The
lower chamber was filled with complete medium. Cell dishes were incubated at 37 °C in 5%
CO_2 and 95% air for 24 h. Nonmigrating cells on the upper side of the filter were wiped-off
and migrating cells on the reverse side of the filter were stained with 0.1% crystal violet in
20% methanol for 15 min, counted, and photographed. Cell migration was quantified by

counting the number of stained nuclei in five individual fields in each transwell membrane in triplicate. Each experiment was repeated three times.

Wound healing assay

8505C and HTH74 cells were grown up to 80% confluence; a wound of ~300 μm width was inflicted to the cell monolayer with a sterile pipette tip. The culture medium was changed to remove nonadherent cells. The progress of wound closure (healing) was monitored and microphotographs of ×10 magnification were taken immediately and 24 h after the wound. Pixel densities in the wound areas were measured using the Cella Software (Olympus Biosystem GmbH, Hamburg, Germany) and expressed as percentage of wound closure. The experiment was repeated three times.

Luciferase assay

Cells were transfected with 500 ng of the reporter plasmid DNA (6XCDX2), together with the other required plasmids, using Lipofectamine reagent (Invitrogen) according to manufacturer's instructions. A plasmid expressing the enzyme Renilla luciferase (pRL-null) was used as internal control. In all cases, the total amount of transfected plasmid DNA was normalized by adding empty vector DNA. Forty-eight hours after transfection, Firefly and Renilla luciferase activities were assayed using the Dual-Luciferase Reporter System (Promega Corporation), and the Lumat LB9507 luminometer (EG Berthold, Bad Wildbad, Germany). Each experiment was done in triplicate.

Fluorescence-activated cell sorter analysis

Cells were harvested and fixed in 70% ethanol for 4 h. After washing with PBS, cells were treated with RNase A (100 units/ml) and stained with propidium iodide (25 μg/ml; Sigma–Aldrich) for 30 min. Samples were analyzed with an FACS-CyAN interfaced with the Summit V4.2 Software (Dako, Glostrup, Denmark). Data were analyzed with the Modfit Software (Verity Software House, Topsham, ME, USA).

Orthotopic tumor experiments

Mice experiments were done in the Division of Cancer Biology and Angiogenesis (Program: Human Thyroid Cancers Preclinical and Translational Research) at the Beth Israel Deaconess Medical Center (Boston, MA) in accordance with federal, local, and institutional guidelines. We used an orthotopic mouse model of ATC as described previously (Nucera *et al.* 2009, 2010,2011). Eight mice (4- to 6-week-old severe combined immunodeficient – SCID ICR – female mice, Taconic, USA) were injected in the right mouse thyroid lobe with 8505c ATC cells and randomly divided into two groups (vehicle or thiostrepton) of four mice each. Thiostrepton was dissolved at a concentration of 50 mg/ml in 1% dimethyl sulfoxide (DMSO) in PBS and the drug solution was sonicated for 10 min. Mice were treated by i.p. injection with 500 mg/kg body weight per day of thiostrepton or with vehicle using a Hamilton syringe, twice a week for 3 weeks starting 7 days after orthotopic tumor implantation (early therapeutic intervention model). Thiostrepton-treated mice compared to vehicle-treated mice displayed signs of toxicity in the third week of treatment (e.g. 1.2-fold decrease in body weight and piloerection). Mice were killed and tissue specimens were fixed with 10% buffered formalin phosphate and embedded in paraffin blocks. Histopathology evaluation was performed by an endocrine pathologist (PM Sadow, MGH, Harvard Medical School, Boston) on hematoxylin and eosin (H&E)-stained tissue sections of the orthotopic thyroid tumors, the surrounding perithyroidal tissues, and the lungs. Slides were examined with an Olympus BX41 microscope and the Olympus Q COLOR 5 photo camera (Olympus, Center Valley, PA, USA). For each mouse, the number of metastases was counted as the

number of pleomorphic 8505c cells foci/section of whole lung. The number of metastases found in each mouse was averaged per each group.

Statistical analysis

The two-tailed unpaired Student's *t*-test was used for statistical analysis. All *P* values were two sided and differences were significant when *P* was <0.05. All statistical analysis was carried out using the GraphPad Instat Software program (version 3.06.3; GraphPad, San Diego, CA, USA).

Results

Increased *FOXM1* expression in ATC

We studied the expression of *FOXM1* by immunohistochemistry in a set of 13 normal thyroids, 78 PDCs, and 41 ATCs. Results are reported in Table 1 and representative pictures are shown in Fig. 1. FOXM1 was not detectable in normal thyroid samples. Overall, 45 and 90% of the PDCs and ATCs respectively expressed FOXM1 (*P*=0.0000011 two-tailed Fisher's exact test; relative risk (RR)=0.16; 95% confidence interval (95% CI), 0.063–0.434). High (+++) and/or medium (++) levels of FOXM1 immunoreactivity significantly correlated with the ATC phenotype (17 vs 65% of positively stained PDCs and ATCs respectively; *P*=0.000045 Fisher's exact test; χ^2 Yates value 14.95, *P*=0.00011 and χ^2 Pearson value 16.85, P<0.0001; RR=2.58; 95% CI, 1.59–4.20; Table 1 and Fig. 1). In a very small set of distant metastases of PDC cases to the brain or lung (three cases), we observed that those metastases that exhibited a PDC phenotype expressed FOXM1 (30–50% of the cells) while the metastasis displaying a phenotype (FTC) that was better differentiated than the primary tumor (PDC) was negative for FOXM1 (Supplementary Figure 1, see section on supplementary data given at the end of this article).

Thirty-one out of 119 PDC and ATC cases presented concurrent areas displaying more prominent differentiated features than the rest of the tumor (see Table 2). In 11 (35.5%) of these cases, *FOXM1* expression was restricted to the PDC or ATC areas (Table 2). Twenty-one percent (5/24) of the concurrent PTC foci present in the PDCs and ATCs analyzed displayed low immunoreactivity (5– 25% positive cells) and none showed moderate or high staining levels (Table 2). This figure is consistent with a recent report by Ahmed *et al.* (2012), who reported *FOXM1* expression in 28.4% of PTC. Finally, none of the concurrent FTC foci (n. 3) present in the PDCs and ATCs analyzed expressed FOXM1.

Then, we selected a group of additional WDTCs (FTCs and PTCs) for further analysis. In particular, we selected PTCs belonging to different subtypes and that have infiltrated or not tumor or thyroid capsule. As shown in Supplementary (Table 1), see section on supplementary data given at the end of this article, both FTCs and PTCs resulted negative or disclosed low (+) *FOXM1* expression levels. PTC stain for FOXM1 depended on the specific variant analyzed. According to Ahmed *et al.* (2012), tall-cell variant PTC as well as PTCs with tall-cell areas featured increased positivity compared with the other PTC variants (P=0.027 Fisher's exact test; χ^2 Yates value 4.71, *P*=0.029 and χ^2 Pearson value 6.41, *P*=0.011; RR=1.77; 95% CI, 1.08–2.90). Moreover, a significant correlation was found between *FOXM1* expression and tumor (P=0.017 Fisher's exact test) or thyroid (*P*=0.0045 Fisher's exact test; χ^2 Yates value 7.71, *P*=0.005 and χ^2 Pearson value 9.75, *P*=0.001; RR=2.28; 95% CI, 1.25–4.17) capsule invasion. Instead, no correlation was found between *FOXM1* expression and the presence of lymph node metastases from primary PTCs (*P*=0.30 Fisher's exact test; Supplementary Table 2, see section on supplementary data given at the end of this article). Even when considering selected cases of WDTCs (with a high percentage of infiltrating tumors), we observed that FOXM1 was significantly increased in

ATCs compared with WDTCs (PTCs+FTCs; P=0.000003), PTCs (P=0.0001), and FTCs (P=0.00002).

We performed qRT-PCR analysis on RNA extracted from normal thyroids (16 cases), PTCs (19 cases), PDC (11 cases), and ATCs (15 cases). *FOXM1* mRNA expression was significantly higher in ATC samples compared with normal thyroid (P<0.001), PTCs (P<0.001), and PDCs (P<0.001; Fig. 2A).

FOXM1 gene is located on chromosome 12p13.3 and consists of nine exons, two of which (A1 and A2) are alternatively spliced giving rise to three differentially expressed forms: *FOXM1a* (containing both A1 and A2 exons), *FOXM1c* (containing only A1), and *FOXM1b* (lacking both A1 and A2) (Fig. 2B). Only *FOXM1b* and *FOXM1c* are active as transcription factors because of the lack of the inhibitory sequence encoded by exon A2 (Ye *et al.* 1997). To address the relative expression of the three forms in normal and tumor thyroid tissues (nine samples for each category), we applied RT-PCR and primers specifically designed to amplify the regions containing A1 and A2 exons. These primers generate large or small PCR fragments depending on the presence or not of the targeted exon. In particular, to discriminate between FOXM1a and FOXM1b and c, we used a primer pair (F3 and R3) that produced PCR fragments of 472 and 358 bp respectively depending on the presence of exon A2 (variant *FOXM1a*); to discriminate between *FOXM1b* and *FOXM1a* and *c* variants, we used primers (F2 and R2) that produced PCR fragments of 481 and 436 bp respectively depending on the presence of exon A1 (variants *FOXM1a* and *c*; Fig. 2B). FOXM1b and FOXM1c plasmids were used to generate PCR products as molecular weight controls. Tumor samples predominantly expressed *FOXM1c* (Fig. 2C). Noteworthy, *FOXM1c* was reported to be the variant that more strongly triggers proliferation and invasion of cancer cells (Kim *et al.* 2006). According to the qRT-PCR data, *FOXM1* expression in ATC was more prominent and consistent than in PTC and PDC.

Deregulation of the p53 and PI3K pathways promotes *FOXM1* overexpression in ATC cells

We investigated mRNA and protein levels of FOXM1 in a panel of ATC cell lines. A primary culture of normal thyrocytes, P5, was used as control. ATC cell lines expressed high levels of FOXM1 mRNA (Fig. 3A) and protein (Fig. 3B) compared with normal cells. As for tissue samples, ATC cell lines expressed *FOXM1c* form (Fig. 3A).

Then, we searched for ATC-associated molecular pathways that may trigger FOXM1 upregulation. *FOXM1* has been recently identified as a target of p53-mediated repression, secondary to p21(CIP1/-WAF1)-mediated Rb dephosphorylation and E2F downregulation (Barsotti & Prives 2009, Pandit *et al.* 2009). This event is critical for the maintenance of a stable G2 arrest in response to DNA damage. Thus, we transfected two ATC-derived cell lines, 8505C and HTH74, both harboring *TP53* point mutations (R248G and K286E respectively) with plasmids coding for wild-type p53, p53-R248G (inactive mutant), p21(CIP1/WAF1), E2F1(1–374) (a dominant negative E2F1), and E2F4 (a negative regulator of the E2F family) together with a firefly luciferase reporter (6XCDX2) that contains FOXM1 binding sites and therefore is able to monitor FOXM1 transcriptional activity (Kim *et al.* 2006). As shown in Fig. 4A, adoptive overexpression of p53 wt, p21(CIP1/WAF1), E2F1(1–374), and E2F4 decreased FOXM1 activity, compared with cells transfected with the empty vector (P<0.001), while p53-R248G did not show any significant effect (Fig. 4A). Consistently, *FOXM1* mRNA levels, as measured by qRT-PCR, were reduced in p53 wt-, p21(CIP1/WAF1)-, and E2F4-transfected cells (Fig. 4B).

Thyroid cancer often features constitutive activation of the PI3K/AKT pathway (Garcia-Rostan *et al.* 2005, Saji & Ringel 2010) and this event is more prevalent in ATC than in WDTC (Gimm *et al.* 2000, Garcia-Rostan *et al.* 2005, Saji & Ringel 2010). *FOXO3a*

transcription factor is negatively controlled by AKT and, in turn, *FOXM1* gene expression is negatively regulated by *FOXO3a* in breast cancer (McGovern *et al.* 2009). Thus, we transfected ATC cells with plasmids coding for a dominant negative *AKT* mutant (K179M), wild-type AKT (used as a control), and FOXO3a together with the FOXM1 activity reporter. AKT (K179M) and FOXO3a transfection strongly reduced FOXM1 activity in ATC cells, while wild-type AKT showed no significant effect (Fig. 4A). Accordingly, treatment with LY294002, a chemical PI3K inhibitor, reduced FOXM1-responsive reporter (Fig. 4A) and *FOXM1* mRNA levels (Fig. 4B). Importantly, chemical blockade of the MAPK pathway by the MEK1 inhibitor PD98059 did not recapitulate this event (Fig. 4A).

Based on these findings, we correlated protein expression levels of FOXM1 with those of p53 (an indirect marker suggestive of p53 pathway inactivation), phospho-AKT (pSer473), and pERK (Thr202/Tyr204) by immunohistochemical stain of the ATC/PDC TMAs. In summary, among 41 ATC samples, four scored negative and 37 scored positive for FOXM1; one scored negative and 40 scored positive for pAKT; ten scored negative and 31 scored positive for p53; and 26 scored negative and 15 scored positive for pERK. Among PDC samples, 43 scored negative and 35 scored positive for FOXM1; six scored negative and 72 scored positive for pAKT; 44 scored negative and 34 scored positive for p53; and 48 scored negative and 30 scored positive for pERK. By applying linear regression analysis, a correlation was found between *FOXM1* expression and p53 (P=0.005; Pearson correlation coefficient (ρ) 0.254) or pAKT (P=0.0015; Pearson correlation coefficient (ρ) 0.286) stain but not between FOXM1 and pERK (P=0.2) stain. All together, these findings suggest that loss of p53 and gain of AKT pathways are molecular events driving FOXM1 transcription levels in thyroid cancer.

Downregulation of FOXM1 inhibited ATC cell growth and invasion *in vitro*

We knocked down *FOXM1* expression by siRNA in 8505C and HTH74 and monitored cell counts in triplicate at 48 h. *FOXM1* siRNA but not negative control caused growth inhibition in both cell lines tested (P<0.001; Fig. 5A), parallel to *FOXM1* mRNA knockdown (see below Fig. 5D). This effect was associated with a reduced S phase entry (P<0.05) as well as an accumulation of the cells in the G2 phase of the cell cycle (P<0.05) as shown by FACS analysis (Fig. 5A).

ATC features a highly invasive and metastatic phenotype. FOXM1 promotes the transcription of genes involved in extracellular matrix degradation and motility, thereby acting as a master regulator of metastasization (Raychaudhuri & Park 2011). Thus, we monitored cell motility (wound closure assay) and invasion (transwell chamber assay) upon *FOXM1* knockdown. FOXM1 depletion significantly impaired the capability of ATC cells (8505c and HTH74) to close the wound (P<0.001; Fig. 5B) and to invade through Matrigel (P<0.001; Fig. 5C) when compared to the scrambled control.

Finally, we tested whether pro-mitogenic and -invasive effects were mediated by the transcriptional program induced by FOXM1. Transcriptional effects of *FOXM1* include upregulation of genes involved in cell proliferation and invasion (Laoukili *et al.* 2005). As shown in Fig. 5D, FOXM1 downregulation in ATC cells blunted the expression of mRNAs related to cell cycle as well as invasion such as *CCNB1, PLK1, AURKB, SKP2*, and *PLAU*. Noteworthy, some of these FOXM1 targets have been previously reported to be upregulated in ATC (*SKP2*, Chiappetta *et al.* (2007); *CCNB1*, Ito *et al.* (2002); *AURKB*, Sorrentino *et al.* (2005) and Wiseman *et al.* (2007); and *PLK1*, Nappi *et al.* (2009)).

Pharmacological inhibition of FOXM1-reduced growth and metastasization of ATC cells in an orthotopic mouse model

FOXM1 has been recently considered as a potential therapeutic target for cancer treatment, thanks to the discovery of a group of compounds able to bind it and inhibit its transcriptional activity (Bhat *et al.* 2009). Owing to the breakage of a FOXM1-dependent positive feedback loop, these drugs lead to FOXM1 protein reduction and cell death due to apoptosis (Halasi & Gartel 2009). We first tested whether thiostrepton, the most characterized among them (Radhakrishnan *et al.* 2006, Kwok *et al.* 2008, Hegde *et al.* 2011), was effective at reducing FOXM1 transcriptional activity and protein level in ATC cells. As shown in Supplementary (Figure 2), see section on supplementary data given at the end of this article, thiostrepton treatment reduced in a dose-dependent manner FOXM1 transcriptional activity as well as its protein levels at 48 h of treatment. Furthermore, this led to a reduction of ATC cell viability as measured by cell count at 48 h (Supplementary Figure 2, see section on supplementary data given at the end of this article).

Thus, we used a recently developed orthotopic mouse model of ATC (Nucera *et al.* 2009). This system closely recapitulates human ATC morphology and biological behavior and allows the study of ATC cell growth into their natural environment and their metastatic properties. We injected 8505c cells into the right thyroid lobe of immunocompromised mice and randomly treated them twice weekly with 500 mg/kg body weight per day of thiostrepton or vehicle. Thiostrepton treatment dramatically reduced tumor volume ($P<0.05$; Fig. 6A, B and E). Thyroid tumors in vehicle-treated mice featured a highly invasive phenotype (Fig. 6C and D). In contrast, thyroid tumors in thiostrepton-treated mice showed signs of necrosis and tumor atrophy (Fig. 6F and G). Importantly, while vehicle-treated mice developed numerous metastatic foci in the lungs (Fig. 6H), mice treated with thiostrepton lacked any evidence of lung metastases (Fig. 6I).

Discussion

FOXM1 oncogenic factor is a master regulator of a transcriptional program that includes genes mediating cell proliferation, motility, invasion, and metastasization. In this study, we show that *FOXM1* expression is strongly upregulated in virtually all ATC samples (90%). Recently, *FOXM1* expression was reported to be negatively controlled by p53 and FOXO3a antioncogenic transcriptional factors (Barsotti & Prives 2009, McGovern *et al.* 2009, Pandit *et al.* 2009). Impaired activity of both these tumor suppressors is part of the molecular features of ATC that, indeed, include *p53* loss-of-function as well as *PI3K/AKT* gain-of-function mutations (Smallridge *et al.* 2009, Saji & Ringel 2010). Here, we show that release from p53-and FOXO3a-negative constraints contributes to FOXM1 upregulation in ATC cells in culture and provide immunohistochemical evidence of a correlation between AKT and p53 pathway activity and *FOXM1* expression in thyroid cancer (Fig. 7). Importantly, we show that this pathway is amenable of therapeutic targeting by PI3K chemical inhibitors, drugs that have been recently proposed as potential therapeutic tools in preclinical models of thyroid cancer (Jin *et al.* 2009, 2011, Xing 2010, Liu *et al.* 2011, 2012).

FOXM1c was the FOXM1 splicing variant most abundant in ATC and FOXM1c was reported to be the form endowed with more potent mitogenic and proinvasive effects (Kim *et al.* 2006). We show that ATC cells depend on FOXM1 expression for both proliferation and *in vitro* motility and invasion. Accordingly, FOXM1 ablation downregulated the expression of a set of genes that, in turn, mediates these functions. These findings support a model whereby FOXM1 upregulation may contribute to the locally invasive, metastatic, and mitogenic phenotype of ATC; in turn, release of ATC cells from the normal cell cycle checkpoints may eventually facilitate chromosomal instability, a common feature of ATC (Fig. 7). Importantly, we could validate this model *in vivo* by showing that treatment with

thiostrepton, a natural compound that reduces *Foxm1* transcriptional activity and protein level (Radhakrishnan *et al.* 2006, Kwok *et al.* 2008), strongly reduced tumor burden and abolished metastasization in a thyroid orthotopic ATC mouse model. It should be noted, however, that thiostrepton may mediate these effects also by affecting targets other than FOXM1. Similarly, Ahmed *et al.* (2012) have previously reported that thiostrepton impairs thyroid cancer cell growth and invasion *in vitro*.

Our data represent an extension of the findings recently reported by Ahmed *et al.* (2012), who, studying differentiated thyroid carcinomas, demonstrated that FOXM1 was upregulated in a fraction (28.4%) of PTCs and correlated with aggressive PTC variants (tall-cell) and expression of molecular markers of invasiveness, such as metalloproteases. Here, we show that FOXM1 is significantly increased in ATCs compared with WDTCs (PTCs and/or FTCs) and PDCs, and when considering only the most aggressive thyroid cancer phenotypes (PDCs and ATCs), high and/or moderate levels of FOXM1 were significantly associated with ATCs. Moreover, by studying a selected series of PTC with or without tumor and/or thyroid capsule invasion, we found that FOXM1 levels correlated with a tumor invasive phenotype.

Altogether, these findings suggest that FOXM1 is a molecular determinant of thyroid cancer malignant phenotype and may be exploited as a molecular marker of aggressiveness as well as a molecular target in approaches aimed at inhibiting directly its transcriptional activity or indirectly the pathways sustaining its expression (Fig. 7).

Supplementary Material

Refer to Web version on PubMed Central for supplementary material.

Acknowledgments

References

Ahmad A, Wang Z, Kong D, Ali S, Li Y, Banerjee S, Ali R, Sarkar FH. FoxM1 down-regulation leads to inhibition of proliferation, migration and invasion of breast cancer cells through modulation of extra-cellular matrix degrading factors. Breast Cancer Research and Treatment. 2010; 122:337–346. (doi:10.1007/s10549-009-0572-1). [PubMed: 19813088]

Ahmed M, Uddin S, Hussain AR, Alyan A, Jehan Z, Al-Dayel F, Al-Nuaim A, Al-Sobhi S, Amin T, Bavi P, et al. FoxM1 and its association with matrix metalloproteinases (MMP) signaling pathway in papillary thyroid carcinoma. Journal of Clinical Endocrinology and Metabolism. 2012; 97:E1–E13. (doi:10.1210/jc.2011-1506). [PubMed: 22049175]

Barsotti AM, Prives C. Pro-proliferative FoxM1 is a target of p53-mediated repression. Oncogene. 2009; 28:4295–4305. (doi:10.1038/onc.2009.282). [PubMed: 19749794]

Bhat UG, Halasi M, Gartel AL. Thiazole antibiotics target FoxM1 and induce apoptosis in human cancer cells. PLoS ONE. 2009; 4:e5592. (doi:10.1371/journal.pone.0005592). [PubMed: 19440351]

Chiappetta G, De Marco C, Quintiero A, Califano D, Gherardi S, Malanga D, Scrima M, Montero-Conde C, Cito L, Monaco M, et al. Overexpression of the S-phase kinase-associated protein 2 in thyroid cancer. Endocrine-Related Cancer. 2007; 14:405–420. (doi:10.1677/ERC-06-0030). [PubMed: 17639054]

Curcio F, Ambesi-Impiombato FS, Perrella G, Coon HG. Long-term culture and functional characterization of follicular cells form adult normal human thyroids. PNAS. 1994; 9:9004–9008. (doi:10.1073/pnas.91.19.9004). [PubMed: 8090760]

Frisk T, Foukakis T, Dwight T, Lundberg J, Höög A, Wallin G, Eng C, Zedenius J, Larsson C. Silencing of the PTEN tumor-suppressor gene in anaplastic thyroid cancer. Genes, Chromosomes & Cancer. 2002; 35:74–80. (doi:10.1002/gcc.10098). [PubMed: 12203792]

Garcia-Rostan G, Sobrinho-Simoes M. Poorly differentiated thyroid carcinoma: an evolving entity. Diagnostic Histopathology. 2011; 17:114–123. (doi:10.1016/j.mpdhp.2010.12.001).

Garcia-Rostan G, Zhao H, Camp RL, Pollan M, Herrero A, Pardo J, Wu R, Carcangiu ML, Costa J, Tallini G. Ras mutations are associated with aggressive tumor phenotypes and poor prognosis in thyroid cancer. Journal of Clinical Oncology. 2003; 21:3226–3235. (doi:10.1200/JCO.2003.10.130). [PubMed: 12947056]

Garcia-Rostan G, Costa AM, Pereira-Castro I, Salvatore G, Hernandez R, Hermsem MJ, Herrero A, Fusco A, Cameselle-Teijeiro J, Santoro M. Mutation of the PIK3CA gene in anaplastic thyroid carcinoma. Cancer Research. 2005; 15:10199–10207. (doi:10.1158/0008-5472. CAN-04-4259). [PubMed: 16288007]

Gimm O, Perren A, Weng LP, Marsh DJ, Yeh JJ, Ziebold U, Gil E, Hinze R, Delbridge L, Lees JA, et al. Differential nuclear and cytoplasmic expression of PTEN in normal thyroid tissue, and benign and malignant epithelial thyroid tumors. American Journal of Pathology. 2000; 156:1693–1700. (doi:10.1016/S0002-9440(10)65040-7). [PubMed: 10793080]

Halasi M, Gartel AL. A novel mode of FoxM1 regulation: positive auto-regulatory loop. Cell Cycle. 2009; 8:1966–1967. (doi:10.4161/cc.8.12.8708). [PubMed: 19411834]

Hedinger C, Williams ED, Sobin LH. The WHO histological classification of thyroid tumors: a commentary on the second edition. Cancer. 1989; 63:908–911. (doi: 10.1002/1097-0142(19890301)63:5<908::AID-CNCR2820630520>3.0.CO;2-I). [PubMed: 2914297]

Hegde NS, Sanders DA, Rodrigez R, Balasubramanian S. The transcription factor FOXM1 is a cellular target of the natural product thiostrepton. Nature Chemistry. 2011; 3:725–731. (doi:10.1038/nchem.1114).

Ito Y, Yoshida H, Nakano K, Takamura Y, Kobayashi K, Yokozawa T, Matsuzuka F, Matsuura N, Kuma K, Miyauchi A. Expression of G2-M modulators in thyroid neoplasms: correlation of cyclin A, B1 and cdc2 with differentiation. Pathology, Research and Practice. 2002; 198:397–402. (doi:10.1078/0344-0338-00272).

Jin N, Jiang T, Rosen DM, Nelkin BD, Ball DW. Dual inhibition of mitogen-activated protein kinase kinase and mammalian target of rapamycin in differentiated and anaplastic thyroid cancer. Journal of Clinical Endocrinology and Metabolism. 2009; 94:4107–4112. (doi:10.1210/jc.2009-0662). [PubMed: 19723757]

Jin N, Jiang T, Rosen DM, Nelkin BD, Ball DW. Synergistic action of a RAF inhibitor and a dual PI3K/mTOR inhibitor in thyroid cancer. Clinical Cancer Research: an Official Journal of the American Association for Cancer Research. 2011; 17:6482–6489. (doi: 10.1158/1078-0432.CCR-11-0933). [PubMed: 21831957]

Kalin TV, Wang IC, Ackerson TJ, Major ML, Detrisac CJ, Kalinichenko VV, Lyubimov A, Costa RH. Increased levels of the FoxM1 transcription factor accelerate development and progression of prostate carcinomas in both TRAMP and LADY transgenic mice. Cancer Research. 2006; 66:1712–1720. (doi:10.1158/0008-5472.CAN-05-3138). [PubMed: 16452231]

Kalinichenko VV, Major ML, Wang X, Petrovic V, Kuechle J, Yoder HM, Dennewitz MB, Shin B, Datta A, Raychaudhuri P, et al. Foxm1b transcription factor is essential for development of hepatocellular carcinomas and is negatively regulated by the p19ARF tumor suppressor. Genes and Development. 2004; 18:830–850. (doi:10.1101/gad.1200704). [PubMed: 15082532]

Kim IM, Ackerson T, Ramakrishna S, Tretiakova M, Wang IC, Kalin TV, Major ML, Gusarova GA, Yoder HM, Costa RH, et al. The forkhead box m1 transcription factor stimulates the proliferation

of tumor cells during development of lung cancer. Cancer Research. 2006; 66:2153–2161. (doi: 10.1158/0008-5472.CAN-05-3003). [PubMed: 16489016]

Kondo T, Ezzat S, Asa SL. Pathogenetic mechanisms in thyroid follicular-cell neoplasia. Nature Reviews. Cancer. 2006; 6:292–306. (doi:10.1038/nrc1836).

Korver W, Roose J, Clevers H. The winged-helix transcription factor Trident is expressed in cycling cells. Nucleic Acids Research. 1997; 25:1715–1719. (doi:10.1093/nar/25.9.1715). [PubMed: 9108152]

Kwok JM, Myatt SS, Marson CM, Coombes RC, Constantinidou D, Lam EW. Thiostrepton selectively targets breast cancer cells through inhibition of FOXM1 expression. Molecular Cancer Therapeutics. 2008; 7:2022–2032. (doi:10.1158/1535-7163.MCT-08-0188). [PubMed: 18645012]

Laoukili J, Kooistra MR, Bràs A, Kauw J, Kerkhoven RM, Morrison A, Clevers H, Medema RH. FoxM1 is required for execution of the mitotic programme and chromosomal stability. Nature Cell Biology. 2005; 7:126–136. (doi:10.1038/ncb1217).

Li Q, Zhang N, Jia Z, Le X, Dai B, Wei D, Huang S, Tan D, Xie K. Critical role and regulation of transcription factor FoxM1 in human gastric cancer angiogenesis and progression. Cancer Research. 2009; 69:3501–3509. (doi:10.1158/0008-5472.CAN-08-3045). [PubMed: 19351851]

Liu M, Dai B, Kang SH, Ban K, Huang FJ, Lang FF, Aldape KD, Xie TX, Pelloski CE, Xie K, et al. FoxM1B is overexpressed in human glioblastomas and critically regulates the tumorigenicity of glioma cells. Cancer Research. 2006; 66:3593–3602. (doi:10.1158/0008-5472.CAN-05-2912). [PubMed: 16585184]

Liu R, Liu D, Trink E, Bojdani E, Ning G, Xing M. The Akt-specific inhibitor MK2206 selectively inhibits thyroid cancer cells harboring mutations that can activate the PI3K/Akt pathway. Journal of Clinical Endocrinology and Metabolism. 2011; 96:E577–E585. (doi:10.1210/jc.2010-2644). [PubMed: 21289267]

Liu R, Liu D, Xing M. The Akt Inhibitor MK2206 synergizes, but perifosine antagonizes, the BRAFV600E inhibitor PLX4032 and the MEK1/2 inhibitor AZD6244 in the inhibition of thyroid cancer cells. Journal of Clinical Endocrinology and Metabolism. 2012; 97:E173–E182. (doi: 10.1210/jc.2011-1054). [PubMed: 22090271]

McGovern UB, Francis RE, Peck B, Guest SK, Wang J, Myatt SS, Krol J, Kwok JM, Polychronis A, Coombes RC, et al. Gefitinib (Iressa) represses FOXM1 expression via FOXO3a in breast cancer. Molecular Cancer Therapeutics. 2009; 8:582–591. (doi:10.1158/1535-7163.MCT-08-0805). [PubMed: 19276163]

Miller KA, Yeager N, Baker K, Liao XH, Refetoff S, Di Cristofano A. Oncogenic Kras requires simultaneous PI3K signaling to induce ERK activation and transform thyroid epithelial cells *in vivo*. Cancer Research. 2009; 69:3689–3694. (doi:10.1158/0008-5472.CAN-09-0024). [PubMed: 19351816]

Nappi TC, Salerno P, Zitzelsberger H, Carlomagno F, Salvatore G, Santoro M. Identification of Polo-like kinase 1 as a potential therapeutic target in anaplastic thyroid carcinoma. Cancer Research. 2009; 69:1916–2223. (doi:10.1158/0008-5472.CAN-08-1693). [PubMed: 19223553]

Nikiforov YE, Nikiforova MN. Molecular genetics and diagnosis of thyroid cancer. Nature Reviews. Endocrinology. 2011; 7:569–580. (doi:10.1038/nrendo.2011.142).

Nikiforova MN, Kimura ET, Gandhi M, Biddinger PW, Knauf JA, Basolo F, Zhu Z, Giannini R, Salvatore G, Fusco A, et al. BRAF mutations in thyroid tumors are restricted to papillary carcinomas and anaplastic or poorly differentiated carcinomas arising from papillary carcinomas. Journal of Clinical Endocrinology and Metabolism. 2003; 88:5399–5404. (doi:10.1210/jc. 2003-030838). [PubMed: 14602780]

Nucera C, Nehs MA, Mekel M, Zhang X, Hodin R, Lawler J, Nose V, Parangi S. A novel orthotopic mouse model of human anaplastic thyroid carcinoma. Thyroid. 2009; 19:1077–1084. (doi:10.1089/ thy.2009.0055). [PubMed: 19772429]

Nucera C, Porrello A, Antonello ZA, Mekel M, Nehs MA, Giordano TJ, Gerald D, Benjamin LE, Priolo C, Puxeddu E, et al. B-Raf(V600E) and thrombospondin-1 promote thyroid cancer progression. PNAS. 2010; 107:10649–10654. (doi:10.1073/pnas.1004934107). [PubMed: 20498063]

Nucera C, Nehs MA, Nagarkatti SS, Sadow PM, Mekel M, Fischer AH, Lin PS, Bollag GE, Lawler J, Hodin RA, et al. Targeting BRAFV600E with PLX4720 displays potent antimigratory and anti-invasive activity in preclinical models of human thyroid cancer. Oncologist. 2011; 16:296–309. (doi:10.1634/theoncologist.2010-0317). [PubMed: 21355020]

Pandit B, Halasi M, Gartel AL. p53 negatively regulates expression of FOXM1. Cell Cycle. 2009; 8:3425–3427. (doi:10.4161/cc.8.20.9628). [PubMed: 19806025]

Radhakrishnan SK, Bhat UG, Hughes DE, Wang IC, Costa RH, Gartel AL. Identification of a chemical inhibitor of the oncogenic transcription factor forkhead box M1. Cancer Research. 2006; 66:9731–9735. (doi:10.1158/0008-5472.CAN-06-1576). [PubMed: 17018632]

Raychaudhuri P, Park HJ. FoxM1: a master regulator of tumor metastasis. Cancer Research. 2011; 71:4329–4333. (doi:10.1158/0008-5472.CAN-11-0640). [PubMed: 21712406]

Ricarte-Filho JC, Ryder M, Chitale DA, Rivera M, Heguy A, Ladanyi M, Janakiraman M, Solit D, Knauf JA, Tuttle RM, et al. Mutational profile of advanced primary and metastatic radioactive iodine-refractory thyroid cancers reveals distinct pathogenetic roles for BRAF, PIK3CA, and AKT1. Cancer Research. 2009; 69:4885–4893. (doi:10.1158/0008-5472.CAN-09-0727). [PubMed: 19487299]

Saji M, Ringel MD. The PI3K–Akt–mTOR pathway in initiation and progression of thyroid tumors. Molecular and Cellular Endocrinology. 2010; 321:20–28. (doi:10.1016/j. mce.2009.10.016). [PubMed: 19897009]

Salvatore G, Nappi TC, Salerno P, Jiang Y, Garbi C, Ugolini C, Miccoli P, Basolo F, Castellone MD, Cirafici AM, et al. A cell proliferation and chromosomal instability signature in anaplastic thyroid carcinoma. Cancer Research. 2007; 67:10148–10158. (doi:10.1158/0008-5472.CAN-07-1887). [PubMed: 17981789]

Santarpia L, El-Naggar AK, Cote GJ, Myers JN, Sherman SI. Phosphatidylinositol 3-kinase/akt and ras/raf–mitogen-activated protein kinase pathway mutations in anaplastic thyroid cancer. Journal of Clinical Endocrinology and Metabolism. 2008; 93:278–284. (doi:10.1210/jc.2007-1076). [PubMed: 17989125]

Schweppe RE, Klopper JP, Korch C, Pugazhenthi U, Benezra M, Knauf JA, Fagin JA, Marlow LA, Copland JA, Smallridge RC, et al. Deoxyribonucleic acid profiling analysis of 40 human thyroid cancer cell lines reveals cross-contamination resulting in cell line redundancy and misidentification. Journal of Clinical Endocrinology and Metabolism. 2008; 93:4331–4341. (doi:10.1210/jc.2008-1102). [PubMed: 18713817]

Smallridge RC, Marlow LA, Copland JA. Anaplastic thyroid cancer: molecular pathogenesis and emerging therapies. Endocrine-Related Cancer. 2009; 16:17–44. (doi:10.1677/ERC-08-0154). [PubMed: 18987168]

Sorrentino R, Libertini S, Pallante PL, Troncone G, Palombini L, Bavetsias V, Spalletti-Cernia D, Laccetti P, Linardopoulos S, Chieffi P, et al. Aurora B overexpression associates with the thyroid carcinoma undifferentiated phenotype and is required for thyroid carcinoma cell proliferation. Journal of Clinical Endocrinology and Metabolism. 2005; 90:928–935. (doi:10.1210/jc. 2004-1518). [PubMed: 15562011]

Teh MT, Wong ST, Neill GW, Ghali LR, Philpott MP, Quinn AG. FOXM1 is a downstream target of Gli1 in basal cell carcinomas. Cancer Research. 2002; 62:4773–4780. [PubMed: 12183437]

Volante M, Collini P, Nikiforov YE, Sakamoto A, Kakudo K, Katoh R, Lloyd RV, LiVolsi VA, Papotti M, Sobrinho-Simoes M, et al. Poorly differentiated thyroid carcinoma: the Turin proposal for the use of uniform diagnostic criteria and an algorithmic diagnostic approach. American Journal of Surgical Pathology. 2007; 31:1256–1264. (doi:10.1097/PAS.0b013e3180309e6a). [PubMed: 17667551]

Wang Z, Banerjee S, Kong D, Li Y, Sarkar FH. Downregulation of forkhead box M1 transcription factor leads to the inhibition of invasion and angiogenesis of pancreatic cancer cells. Cancer Research. 2007; 67:8293–8300. (doi:10.1158/0008-5472.CAN-07-1265). [PubMed: 17804744]

Wiseman SM, Masoudi H, Niblock P, Turbin D, Rajput A, Hay J, Bugis S, Filipenko D, Huntsman D, Gilks B. Anaplastic thyroid carcinoma: expression profile of targets for therapy offers new insights for disease treatment. Annals of Surgical Oncology. 2007; 14:719–729. (doi:10.1245/s10434-006-9178-6). [PubMed: 17115102]

Wonsey DR, Follettie MT. Loss of the forkhead transcription factor FoxM1 causes centrosome amplification and mitotic catastrophe. Cancer Research. 2005; 65:5181–5189. (doi: 10.1158/0008-5472.CAN-04-4059). [PubMed: 15958562]

Wreesmann VB, Ghossein RA, Patel SG, Harris CP, Schnaser EA, Shaha AR, Tuttle RM, Shah JP, Rao PH, Singh B. Genome-wide appraisal of thyroid cancer progression. American Journal of Pathology. 2002; 161:1549–1556. (doi:10.1016/S0002-9440(10)64433-1). [PubMed: 12414503]

Wu G, Mambo E, Guo Z, Hu S, Huang X, Gollin SM, Trink B, Ladenson PW, Sidransky D, Xing M. Uncommon mutation, but common amplifications, of the PIK3CA gene in thyroid tumors. Journal of Clinical Endocrinology and Metabolism. 2005; 90:4688–4693. (doi:10. 1210/jc.2004-2281). [PubMed: 15928251]

Xing M. Genetic alterations in the phosphatidylinositol-3 kinase/Akt pathway in thyroid cancer. Thyroid. 2010; 20:697–706. (doi:10.1089/thy.2010.1646). [PubMed: 20578891]

Ye H, Kelly TF, Samadani U, Lim L, Rubio S, Overdier DG, Roebuck KA, Costa RH. Hepatocyte nuclear factor 3/fork head homolog 11 is expressed in proliferating epithelial and mesenchimal cells of embryonic and adult tissues. Molecular and Cellular Biology. 1997; 17:31626–31641.
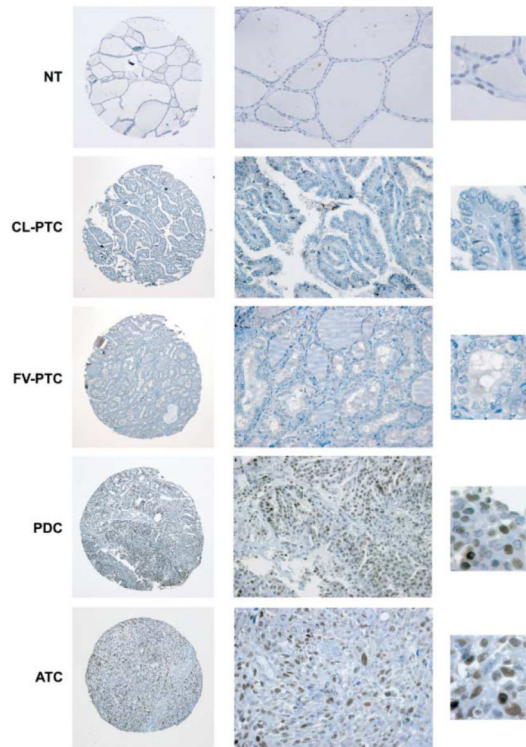
Figure 1.
Immunohistochemical analysis of *FOXM1* expression in human thyroid tissue samples. Representative images of normal thyroid (NT), classic variant-PTC (CL-PTC), follicular variant-PTC (FV-PTC), PDC, and ATC biopsies stained with a rabbit polyclonal anti-FOXM1 antibody. Whole tissue cores (left, 10×) and zoom-in of areas present within these particular cores (center, 40× and right, 100×), illustrating the nuclear features and FOXM1 staining pattern, are shown. The NT, CL-PTC, and FV-PTC sections are negative for FOXM1, whereas the PDC and ATC sections disclose diffuse, medium/moderate (++), and high/ strong (+++) nuclear immunoreactivity respectively.
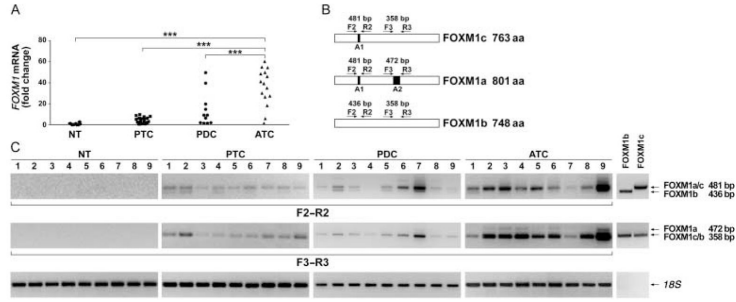
Figure 2.
FOXM1 is overexpressed at the mRNA level in human anaplastic thyroid carcinoma samples. (A) Quantitative RT-PCR showing increased *FOXM1* expression in ATC (15 cases) compared with normal thyroid (16 cases), PTC (19 cases), and PDC (11 cases) samples. Tumor expression values are reported as fold changes with respect to the average expression in normal samples measured with ΔCt method, after normalization for RNA polymerase 2 (***$P<0.001$). (B) Schematic representation of the three alternatively spliced FOXM1 variants (a, b, and c) and the PCR primers used to detect the presence of alternatively spliced exons A1 and A2. (C) RT-PCR to show relative expression levels of the three *FOXM1* forms in normal thyroids, PTCs, PDCs, and ATCs (nine samples for each category). Plasmids encoding FOXM1b and FOXM1c were used as PCR templates to generate molecular weight controls for the presence or the absence of exon A1 (primers F2/R2) or exon A2 (primers F3/R3). Arrows indicate expected migration for PCR products containing (variants *FOXM1a* and *FOXM1c*) or lacking (*FOXM1b*) exon A1 and for PCR products containing (*FOXM1a*) or lacking (*FOXM1b* and *FOXM1c*) exon A2. The molecular weight of the PCR products is shown on the right. Levels of *18S* rRNA were measured for normalization.
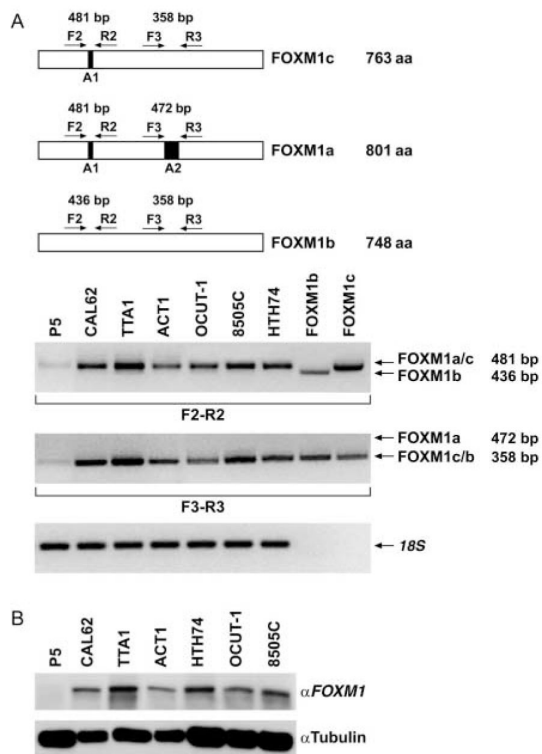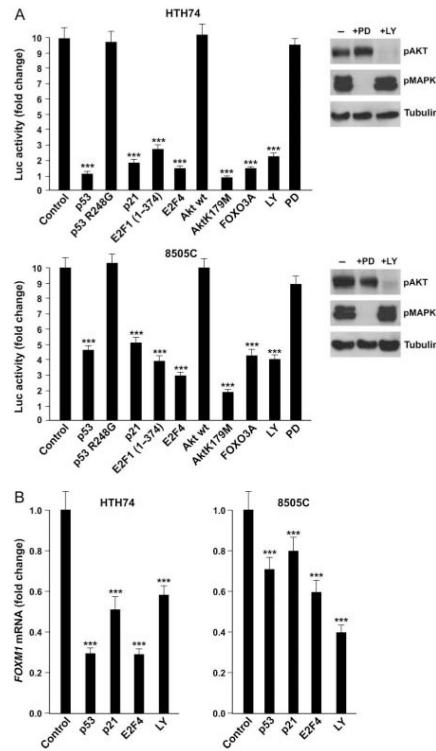
Figure 3.
FOXM1 is overexpressed at the mRNA and protein level in ATC cells. (A) Semiquantitative RT-PCR showing increased levels of *FOXM1c* in ATC cells compared with normal thyrocytes (P5; see legend to Fig. 2). Levels of *18S* rRNA were measured for normalization. (B) Western blot analysis showing increased protein expression of *FOXM1* in ATC cells compared with P5 control. Tubulin was used for normalization. These results are representative of at least three independent experiments.

Figure 4.
FOXM1 in ATC cells is controlled by the p53 and PI3K pathways. (A) The indicated ATC cells were co-transfected with the indicated expression vectors (or the empty vector as control) together with 6XCDX2 containing six copies of the FOXM1 binding site fused to firefly luciferase. Alternatively, as indicated, cells were treated for 48 h with the PI3K inhibitor LY294002 or the MEK1 inhibitor PD98059. Cells were co-transfected with Renilla luciferase for normalization. Normalized luciferase levels are reported as average results of three independent experiments with bars illustrating 95% confidence intervals. Reporter activity in empty vector-transfected cells was arbitrary set at 10 (***P<0.001). Western blot analysis of AKT and MAPK phosphorylation after PD98059 and LY294002 treatment is shown on the right. (B) *FOXM1* mRNA expression levels were measured in the indicated ATC cells 72 h after transfection with the indicated plasmids or treatment with LY294002. The average results of three independent experiments are reported together with 95% confidence intervals. *FOXM1* expression in mock-transfected cells was arbitrary set at 1.0 (***P<0.001).
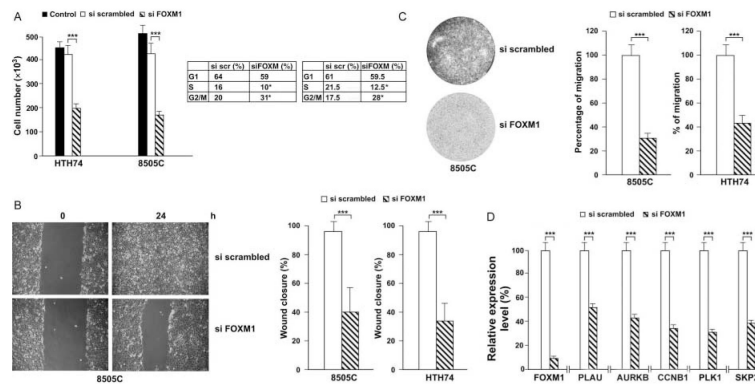
Figure 5.
Effect of FOXM1 silencing on ATC cell growth, migration, and invasion. (A) ATC cells were transfected with either *FOXM1* siRNA or the negative control siRNA or left untransfected. Cells were harvested at 48 h and counted. Values represent the average of triplicate experiments with bars indicating 95% confidence intervals (***$P<0.001$). FACS analysis of siFOXM1 or negative control (siSCR)-transfected 8505c and HTH74 cells is shown together with the mean percentage of cells in G1, S, and G2/M cell cycle phases. Values represent the average of triplicate experiments (*$P<0.05$). (B) 8505C and HTH74 cells, transfected with either *FOXM1* siRNA or the negative control, were plated at confluence and scratch wounds were inflicted. Cell plates were photographed immediately after wound incision and 24 h later. Photographs were taken at 10× magnification. Pixel densities in the wound areas were measured and expressed as percentage of wound closure, where 100% is the value obtained at 10 h for control cells. The average results of three experiments are reported with bars representing 95% confidence intervals (***$P<0.001$). (C) 8505C and HTH74 cells, transfected with either *FOXM1* siRNA or the negative control, were plated in transwells coated with Matrigel. Migration through Matrigel was measured by staining migrated cells with Giemsa. The average results of three experiments are reported with bars representing 95% confidence intervals (***$P<0.001$). D) RNA was extracted from 8505C cells, transfected with either *FOXM1* siRNA or the negative control, and quantitative RT-PCR assays were performed to detect expression levels of the indicated mRNAs. Levels of actin were measured for normalization.
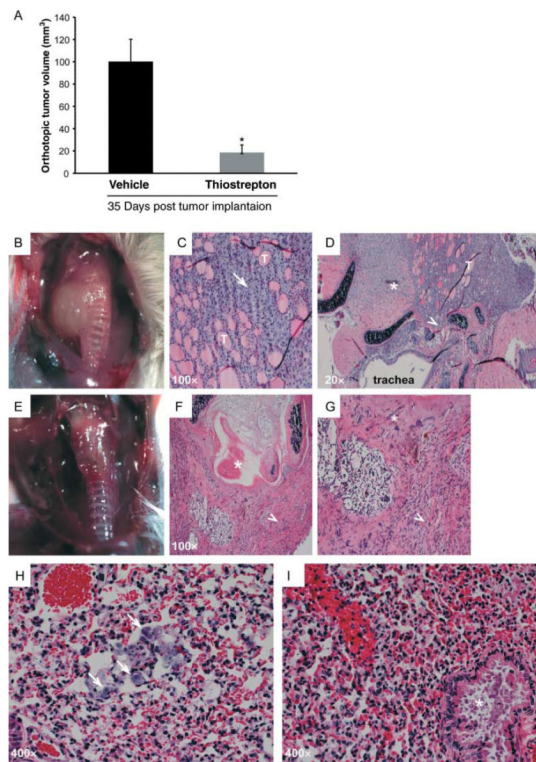
Figure 6.
Thiostrepton treatment reduces ATC cell growth and metastasization *in vivo*. Eight mice were injected orthotopically in the right thyroid lobe with 8505c cells and randomly divided in two groups. Starting 7 days after orthotopic tumor implantation, mice were treated by i.p. injection of thiostrepton or vehicle twice a week for 3 weeks. (A) Thiostrepton-treated mice showed a significant decrease in thyroid tumor volume (18.5 ± 6.8 mm^3) compared with control mice (100 ± 19.9 mm^3) (*P<0.05). (B, C, D, E, F and G) Gross and H&E representative images of thyroids from thiostrepton-treated (E, F and G) or control (B, C and D) mice. In control mice, aggressive ATC (arrow) infiltrating residual thyroid follicles (T), with extra-thyroid extension into skeletal muscle (asterisk) and tracheal cartilage (arrowhead), are visible. In thiostrepton-treated mice, tumors were smaller and round shaped and had histological evidence of atrophy (arrowheads), intratracheal necrosis, and peritracheal fibrosis (asterisks). (H and I) H&E images of lung metastases. In control mice (H), eight to ten pleomorphic cell foci/lung sections (arrows) were counted. In thiostrepton-treated mice (I), no apparent lung metastasis was detected (asterisk: bronchus).
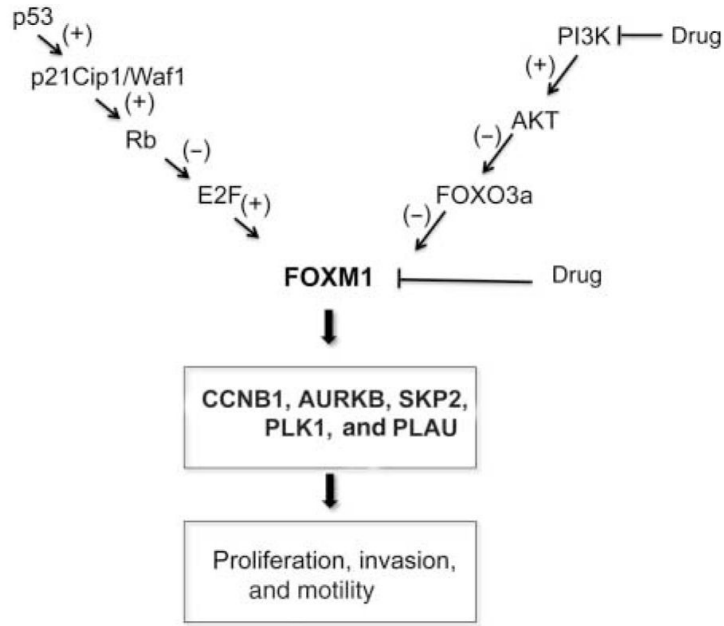
Figure 7.
A model for FOXM1's role in thyroid cancer. Schematic representation of the molecular pathways linked to FOXM1 upregulation in ATC (+ and − refer to activating or inhibitory signals respectively) and gene targets whose expression is stimulated by FOXM1. This pathway can be therapeutically targeted at multiple levels; as shown here and in Ahmed *et al.* (2012), these levels include FOXM1 itself (thiostrepton) and PI3K (LY294002).

Table 1

FOXM1 expression by immunohistochemistry in poorly differentiated thyroid carcinoma (PDC) and anaplastic thyroid carcinoma (ATC)

	Number of cases in each category (percentage of stained target cells)			
Sample diagnosis	Negative (–)	Low/weak (+)	Medium/moderate (++)	High/strong (+++)
Normal thyroid (13 cases)	13 (100%)	0 (0%)	0 (0%)	0 (0%)
PDC (78 cases-347 cores)[a]	43 (55.1%)	29 (37.2%)	6 (7.7%)	0 (0%)
ATC (41 cases-192 cores)[a]	4 (9.7%)	13 (31.7%)	12 (29.3%)	12 (29.3%)

–, <5% of cells positive for nuclear *FOXM1* expression; +, 5– 25% of cells positive for nuclear *FOXM1* expression; ++, >25–<50% of cells positive for nuclear *FOXM1* expression; +++, 50% of cells positive for nuclear *FOXM1* expression.

[a]To improve the representativity of the expression analysis, two to six core biopsies of 1 mm in diameter, from different regions of the same specimen or different blocks of the same tumor, were included in the TMAs.

Table 2

FOXM1 expression in concurrent differentiated thyroid carcinoma foci present within PDCs and ATCs

	FOXM1 staining score[a]		
Patient number	**Concurrent WDTC component**		**Prevailing PDC/ATC component**
1	(–) FV-PTC		(–) PDC
2	(–) FV-PTC		(–) PDC
3	(–) FV-PTC		(+)PDC
4	(+) CL-PTC		(+)PDC
5	(+) FV-PTC		(+)PDC
6	(–) FTC		(+)PDC
7	(–) FV-PTC		(–) PDC
8	(–) CL-PTC with focal tall-cell features		(–) PDC
9	(–) FV-PTC		(–) PDC
10	(–) TCV-PTC		(–) PDC
11	(–) FV-PTC		(+)PDC
12	(–) FTC Hürthle		(+)PDC
13	(–) FV-PTC		(–) PDC
14	(–) Solid PTC		(+)PDC
15	(–) FV-PTC		(–) PDC
16	(C) Mixed-PTC with focal tall-cell features		(+)PDC
17	(–) CL-PTC with focal tall-cell features		(+)PDC
18	(–) Solid PTC		(–) PDC
19	(–) FV-PTC		(–) PDC
20	(–) FV-PTC		(–) PDC
21	(–) FV-PTC		(–) PDC
22	(–) FV-PTC	(–) PDC	(+) ATC
23	(–) FV-PTC	(–) PDC	(+) ATC
24	(+) PDC		(+) ATC
25	(+) PDC		(+) ATC
26	(+) TCV-PTC progressing to PDC		(+) ATC
27	(–) FV-PTC		(+++) ATC
28	(–) PDC		(++) ATC
29	(+) FV-PTC		(+++) ATC
30	(–) FTC Hürthle		(+++) ATC
31	(++) PDC		(++) ATC

The concurrent better differentiated thyroid carcinoma components present within poorly differentiated thyroid carcinomas (PDCs) and anaplastic thyroid carcinomas (ATCs) included well-differentiated follicular thyroid carcinoma (FTC), follicular variant of papillary thyroid carcinoma (FV-PTC), classic papillary thyroid carcinoma (CL-PTC), mixed papillary thyroid carcinoma (FV-PTC+CL-PTC), solid PTC, and tall-cell variant of PTC (TCV-PTC).

[a]Score is reported as in Table 1.